A preliminary evaluation of the correlation between regional energy phosphates and resting state functional connectivity in depression

NeuroImage: Clinical 9 (2015) 348–354

Contents lists available at ScienceDirect

NeuroImage: Clinical

journal homepage: www.elsevier.com/locate/ynicl

A preliminary evaluation of the correlation between regional energy phosphates and resting state functional connectivity in depression

Chun S. Zuo[a,b,*], Pan Lin[a,b,1], Gordana Vitaliano[a,b], Kristina Wang[a], Rosemond Villafuerte[a], Scott E. Lukas[a,b]

[a] McLean Imaging Center, McLean Hospital, Belmont, MA 02478, USA
[b] Harvard Medical School, Belmont, MA 02478, USA

ARTICLE INFO

Article history:
Received 22 June 2015
Received in revised form 24 August 2015
Accepted 31 August 2015
Available online 5 September 2015

Keywords:
Functional connectivity
Energy phosphates
Correlation
Depression

ABSTRACT

Impaired brain energy metabolism is among the leading hypotheses in the pathogenesis of affective disorders and linking energy phosphates with states of tissue-function activity is a novel and non-invasive approach to differentiate healthy from unhealthy states. Resting state functional MRI (fMRI) has been established as an important tool for mapping cerebral regional activity and phosphorous chemical shift imaging (^{31}P CSI) has been applied to measure levels of energy phosphates and phospholipids non-invasively in order to gain insight into the possible etiology of affective disorders. This is an initial attempt to identify the existence of a correlation between regional energy phosphates and connectivity at nodes of the posterior default mode network (DMN). Resting state fMRI in conjunction with ^{31}P 2D CSI was applied to 11 healthy controls and 11 depressed patients at 3 T. We found that differences between the two groups exist in correlation of lateral posterior parietal cortex functional connectivity and regional Pi/PCr. Results of this study indicate that resting-state-fMRI-guided ^{31}P CSI can provide new insight into depression via regional energy phosphates and functional connectivity.

1. Introduction

Mitochondrial dysfunction, including damage to the electron transport chain, has been suggested to be an important factor in a range of neuropsychiatric disorders such as bipolar disorder (BPD), depression, and schizophrenia (MacDonald et al., 2006; Kato and Kato, 2000; Cataldo et al., 2010). This implicates involvement of abnormal energetics in affective disorders, which can be quantified using ^{31}P MRS to measure brain levels of phospholipids and high-energy phosphates and gain insight into the status of these metabolites and possible mechanisms of the disorders (Moore et al., 1997; Kato and Kato, 2000). Much progress has been made in collecting *static* levels of the ^{31}P metabolites from participants while resting in the scanner in conjunction with regional segmented tissue composition (Hetherington et al., 2001). Previous studies on skeletal muscle exercise have also demonstrated a close coupling between work output and regional energy phosphates and how normal and disease differed from each other in performance (Arnold et al., 1984; Chance et al., 1985). This motivates effort to look into paradigms of ^{31}P MRS in conjunction with visual stimulation (Chen et al., 1997) or medications even though applications of these paradigms have their own limitations.

Specifically, within physiological range, the changes in brain energy metabolites due to stimulation or tasks could be relatively small and regional as the brain is operating at nearly full capacity of its energy sources even at resting state (Shulman et al., 2004; Raichle and Mintun, 2006). Furthermore, the long data acquisition time of ^{31}P MRS requires a lengthy stimulation or task, which could increase the probability of unwanted motion artifact. These issues motivated us to collect and examine energy phosphates that may be associated with resting state functional connectivity in patients with affective disorders.

Resting state functional connectivity (RSFC) of the human brain has received an enormous amount of attention in recent years for its involvement in the intrinsic operation of the brain. fMRI studies have found that the default mode network (DMN) is "activated" during resting state but "deactivated" while performing tasks (Shulman et al., 1997; Raichle et al., 2001; Corbetta and Shulman, 2002). This network has been associated with processes ranging from attention lapses to clinical disorders like anxiety (Weissman et al., 2006; Buckner et al., 2008; Castellanos et al., 2008). With resting state functional MRI (fMRI), researchers have recently discovered significant abnormalities in altered spatial distribution and fluctuation frequencies of functional connectivity in the brain of people with affective disorders compared to healthy controls (Ongur et al., 2010; Chai et al., 2011). Note that brain regions within the DMN have a correlated time course of fMRI signals. The higher the degree of the correlation, the higher the functional connectivity.

* Corresponding author at: MR Imaging Center, McLean Hospital, 115 Mill Street, Belmont, MA 02478, USA. Tel.: +1 617 855 3277; fax: +1 617 855 2770.
E-mail address: chun@mclean.harvard.edu (C.S. Zuo).
[1] Present Address: Key Laboratory of Biomedical Information Engineering of Education Ministry, Institute of Biomedical Engineering, Xi'an Jiaotong University, No. 28, Xianining West Road, Xi'an 710049, Shanxi-Province, P.R. China.

http://dx.doi.org/10.1016/j.nicl.2015.08.020

^{31}P MRS can directly measure regional levels of ATP, PCr, Pi, and phospholipid metabolites with a spatial resolution of several cubic centimeters per voxel (Hetherington et al., 2001). Phosphocreatine (PCr), glycolysis, and oxidative phosphorylation in mitochondria are the main energy sources that support brain function and activity. Net adenosine triphosphate (ATP) is generated from glycolysis and oxidative phosphorylation via inorganic phosphate (Pi) and the PCr/creatine (Cr) energy reservoirs provide a buffering effect. The majority of brain ATP is synthesized via oxidative phosphorylation, the ATP source with endurance capacity. PCr and glycolysis, on the other hand, respond quickly to increases in ATP utilization due to enhanced neural activity (Erecinska and Silver, 1989). When PCr responds to an increase in ATP utilization, the level of PCr decreases and the levels of Pi and the Pi/PCr ratio increase. During muscle exercise, higher Pi/PCr ratio is associated with higher work output.

We hypothesize that DMN connectivity may be associated with regional metabolic activity, which may involve metabolites such as GABA and regional energy phosphates. The former has recently been explored extensively (Northoff et al., 2007; Muthukumaraswamy et al., 2009; Donahue et al., 2010; Hu, Chen et al., 2013) but the latter has not been studied, making the present approach the first to address this issue using MRS. We have recently investigated the feasibility of using ^{31}P MRS in conjunction with resting state fMRI in mapping regional energy phosphates associated with functional connectivity at the nodes of the posterior DMN. This report details the results of the preliminary study.

2. Materials & methods

2.1. Participants

Under protocols approved by the McLean Hospital Institutional Review Board (IRB), 11 depressed patients (5 males/6 females, age: 61 ± 8, HAM-D = 21.6 ± 3.2, YMRS = 4.6 ± 3.7) (Table 1), two of them were diagnosed with major depressive disorder (MDD) and nine with BPD depression, were recruited to participate in this study. Eleven age- and sex-matched healthy volunteers (5m/6f, age: 56 ± 8, HAM-D (Hamilton Depression Rating Scale (Hamilton, 1960)) = 0.6, YMRS (Young Mania Rating Scale (Young et al., 1978)) = 0.5 ± 0.8) served as healthy controls. All participants provided written informed consent before participating and had no MRI-related contraindications. All patients were currently on stable doses of medication and included the following: MDD patients were taking quetiapine, sertraline, trazodone and/or venlafaxine. All BPD patients were taking either a mood stabilizer (lithium and/or lamotrigine), an atypical antipsychotic (quetiapine, aripiprazole, risperidone, asenapine), SSRIs (sertraline, trazodone, fluoxetine) or other antidepressant (buproprion, imipramine). In addition, many patients were prescribed a variety of medications to treat hypertension, type 2 diabetes, GERD, thyroid disease, and/or high cholesterol. No participants were on medications or supplements, such as CoQ10, that may alter energy state. Among them, ten depressed patients and ten healthy controls (HC) completed both resting state fMRI and ^{31}P 2D chemical shift imaging (CSI) data collection.

2.2. Resting state fMRI data acquisition

The resting state BOLD MR images were collected on a 3 T whole body MR scanner (TIM Trio, Siemens AG, Germany) using a 32-channel head array. During the resting state imaging, participants were instructed to lie still with their eyes open in low-level illumination without fixation for approximately 9 min. No cognitive tasks were performed before or during the MR study. The BOLD images were obtained with a T_2^*- weighted echo planar imaging (EPI) sequence. Acquisition parameters include TR/TE = 2200/30 ms, 4 dummy scans, flip angle = 90°, and field of view = 224 × 224 mm^2 with a 64 × 64 acquisition matrix, yielding a voxel size of 3.5 × 3.5 × 3.5 mm^3. We acquired 35 contiguous axial functional slices of 3.5 mm thickness without a gap to cover the brain for 240 time points during the resting state fMRI data collection. The first 4 time points of the scan were not included in the data analysis to allow global image intensity to reach steady state.

Table 1
Demographic and mood characteristics.

Group	BPD/MDD	HC	p
Sex (m/f)	5m/6f	5m/6f	
Age (year)	61.0 ± 8.0	56.4 ± 8.4	NS
Illness duration (years)	37.8 ± 9.6		
Ham-D	21.6 ± 3.2	0.4 ± 0.8	<0.01
YMRS	4.6 ± 3.7	0.2 ± 0.6	NS

Note: NS = not significant.

2.3. ^{31}P MRS data acquisition

The ^{31}P 2D CSI was collected with a double-quadrature dual-tuned (proton/phosphorus, ^{1}H/^{31}P) volume head coil (Clinical MR Solutions, LLC, Brookfield, WI, USA) on the same TIM Trio MR scanner used for the resting state fMRI data collection. After shimming to optimize static field homogeneity, a set of 2D ^{31}P CSI data was collected from a graphic prescribed 30-millimeter axial slice across the brain (Fig. 1) using a 2D phase-encoding gradient matrix of 8 × 8 (weighted) and interpolated into 16 × 16 in post-processing. To reduce possible mis-registration due to chemical shift difference, the ^{31}P CSI slice was excited using a 1.28-ms hyperbolic sinc pulse with its excitation bandwidth of 3.55 kHz. Other parameters included flip angle ~52°, TE = 2.3 ms, TR = 2.2 s, FOV = 220, and 18 signal averages for a total data acquisition time (TA) of 6.5 min.

2.4. Resting state fMRI data analysis

Prior to analyzing functional connectivity, motion correction was first performed in 3D realignment with the 3dvolreg function of AFNI (Analysis of Functional NeuroImages, http://afni.nimh.nih.gov/afni/) and a temporal band-pass filter (0.008 Hz < f < 0.1 Hz) was applied to reduce low frequency drift and high frequency physiological noise. Linear regression was also applied to remove nuisance covariates of parameters of rigid body motion, signals from the white matter and ventricle region of interest, and signals from the whole brain mask. In order to better define the DMN node in the posterior cingulate/precuneus cortex (PCC) region in the patients, we used an independent component analysis (ICA) algorithm (MELODIC (Multivariate Exploratory Linear Decomposition into Independent Components) v4.0, one part of FSL (FMRIB's Software Library, http://www.fmrib.ox.ac.uk/fsl) FMRIB Oxford University, UK (Beckmann and Smith, 2004)) to identify DMN components from 60 spatiotemporal independent components and the coordinates of the DMN node in the PCC region.

A PCC seed was defined as a sphere with a radius of 10 mm centered at (0 69 18) (Table 2) and the PCC time series was calculated by averaging the time series of all voxels in the sphere. Correlation maps were generated for each participant by calculating the correlation coefficients, voxel-by-voxel, between the time course of the seed and the time courses of voxels in other brain regions. To test for significant connectivity changes in each participant, the correlation coefficients were converted to Z-scores by using Fisher's r-to-z transformation. For group-level correlation Z-map analysis, we computed a one-sample t-test to yielding a group-averaged Z-score map.

2.5. Correlation of regional activation activities with depression symptom severity

For DMN nodes in the posterior cingulate (PCC) and bilateral posterior parietal cortex (LPPC and RPPC), regional Z-scores were extracted from the Z-score maps with a 10-mm ROI from the corresponding resting state active regions. Because the ^{31}P CSI slice in most of the participants did not cover the DMN regions in the frontal lobe, the data

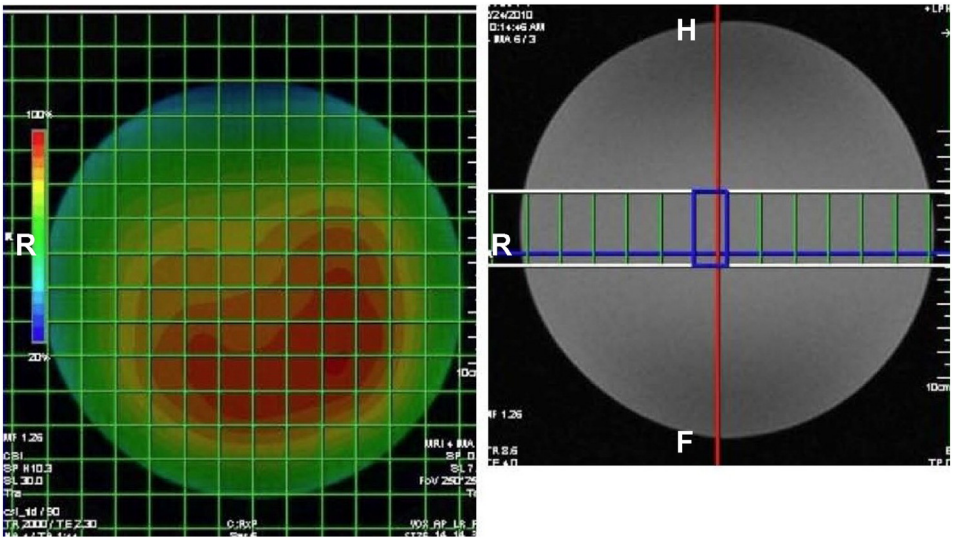

Fig. 1. A color map of Pi signal intensity distribution (left) generated from a ^{31}P 2D CSI of a spherical, *aqueous solution* phantom (right) containing 50-mM KH_2PiO_4 and ~0.5 mM GdDTPA. The CSI was collected in transverse plane in a 3 T scanner using a $^{1}H/^{31}P$ dual tuned head coil. The P_i intensity distribution reflected B_1 distribution of the dual tuned coil at ^{31}P resonance frequency. The Pi signal distribution was collected from a graphic prescribed 30-millimeter axial slice across the brain using a 2D phase-encoding gradient matrix of 8 × 8 (weighted) and interpolated into 16 × 16 in post-processing. The ^{31}P signal was excited using a 1.28-ms hyperbolic sinc pulse with its excitation bandwidth of 3.55 kHz. Other parameters included flip angle ~52°, TE = 2.3 ms, TR = 2.2 s, FOV = 220, and 4 signal averages for a total data acquisition time (TA) of 1.4 min.

analytical strategy was focused in the DMN regions of the PCC and posterior parietal cortex (LPPC and RPPC). In addition, regional Z-scores were also extracted from the extra resting-state active regions of the posterior parietal/occipital lobes which only appeared in the depressed patients ($LPPC_D$ and $RPPC_D$) with a 10-mm ROI (Table 2). Multiple regression analyses were performed to assess the relationship between individual patients' DMN regional Z-scores (functional connectivity) and their symptom severity as assessed by HAM-D. The null hypothesis was tested for each variable of interest using the Student t-test. Statistical significance was defined at an alpha level of $p \le 0.05$, two tailed.

2.6. ^{31}P MRS data processing

The 2D CSI data were post-processed on a satellite console of the MR system for integrals of ^{31}P metabolite signals (Pi, PCr, γ- and α-ATP) voxel-by-voxel. To avoid a relatively large chemical shift misregistration of β-ATP due to its relatively large chemical shift, molecular ATP level (mATP) was calculated by averaging γ- and α-ATP instead of all three components. To minimize the impact of RF B_1 inhomogeneity across the brain at ^{31}P frequency (Fig. 1), metabolic ratios Pi/PCr and Pi/ γATP, instead of comparing absolute levels of the metabolites, were calculated on a voxel-by-voxel basis for comparison. We also examined normalized Pi (calculated as Pi/(Pi + PCr)) as well as normalized PCr (calculated as PCr/(Pi + PCr)) in regions of the DMN. Regions of interest (ROIs) were selected from both-group-overlapped activation regions and depressed-only activation regions in the group correlation maps in the DMN regions of the parietal/occipital lobes (Fig. 2) based on brain anatomy landmark. The Pi/PCr and Pi/γATP ratios were extracted from the CSI voxels at the anatomic locations corresponding the ROIs in the CSI maps superimposed on the anatomic image and the corresponding correlation maps. The Pi/PCr ratios were calculated based on weighting the voxel faction $\sum_i v_i * (Pi/PCr)_i$, where v_i is the voxel faction i and $(Pi/PCr)_i$ is the corresponding Pi/PCr ratio. Similar calculations were applied to the Pi/γATP ratios. The ROI of PCC was a 4-voxel average for both patients and the healthy controls. The ROIs of the LPPC and RPPC were one voxel average, and those of the $LPPC_D$ and $RPPC_D$ were a 2-voxel average for both groups.

Table 2
Location of Z-scores that were extracted from a 10 mm radius sphere.

	Table of ROI coordinates		
Region	x	y	z
PCC	45	34	50
RPPC	−45	63	24
LPPC	42	72	30
$RPPC_D$	−42	48	27
$LPPC_D$	42	63	24

Note: MPFC node of the DMN components was not included in this study because it did not overlap with the slice of the ^{31}P 2D CSI in many participants. Group averaged Z-scores of the ROIs were presented in Fig. 3a and c.

3. Results

3.1. Functional connectivity

Group correlation maps revealed that the resting state active area in the left and right posterior parietal cortex (LPPC and RPPC) of depressed patients was much larger than the area in the healthy controls (Figs. 2 and 3a). Functional connectivity, as measured by group averaged Z-scores, of the healthy controls was noticeably lower than those of the patients in the PCC, LPPC, and RPPC regions (Fig. 3a). The differences of the connectivity reached statistical significance ($p = 0.05$) in the LPPC. More specifically, Z-scores of the healthy controls were 45% lower than that of the patients. The connectivity of the patients in the $LPPC_D$ and $RPPC_D$ regions was significantly higher than those of the controls in the same regions (L: +316%, $p = 0.004$; R: +214%, $p = 0.0103$) (Fig. 3c).

3.2. ^{31}P metabolites

The group averaged Pi/PCr ratios of healthy controls were higher in all DMN regions in the PCC, LPPC, and RPPC (Fig. 3b) as well as the $LPPC_D$ and $RPPC_D$ (Fig. 3c), compared to those of patients, with the difference reaching statistical significance in the LPPC and $LPPC_D$ regions (+19% each in LPPC and $LPPC_D$, $p \le 0.05$). The lower Pi/PCr in the depressed patients was most likely due to reduced Pi because the Pi/γATP ratio was also significantly lower in the regions of the PCC, LPPC, and $LPPC_D$ while pH and PCr/mATP remained statistically similar in all DMN regions of both groups (Table 3).

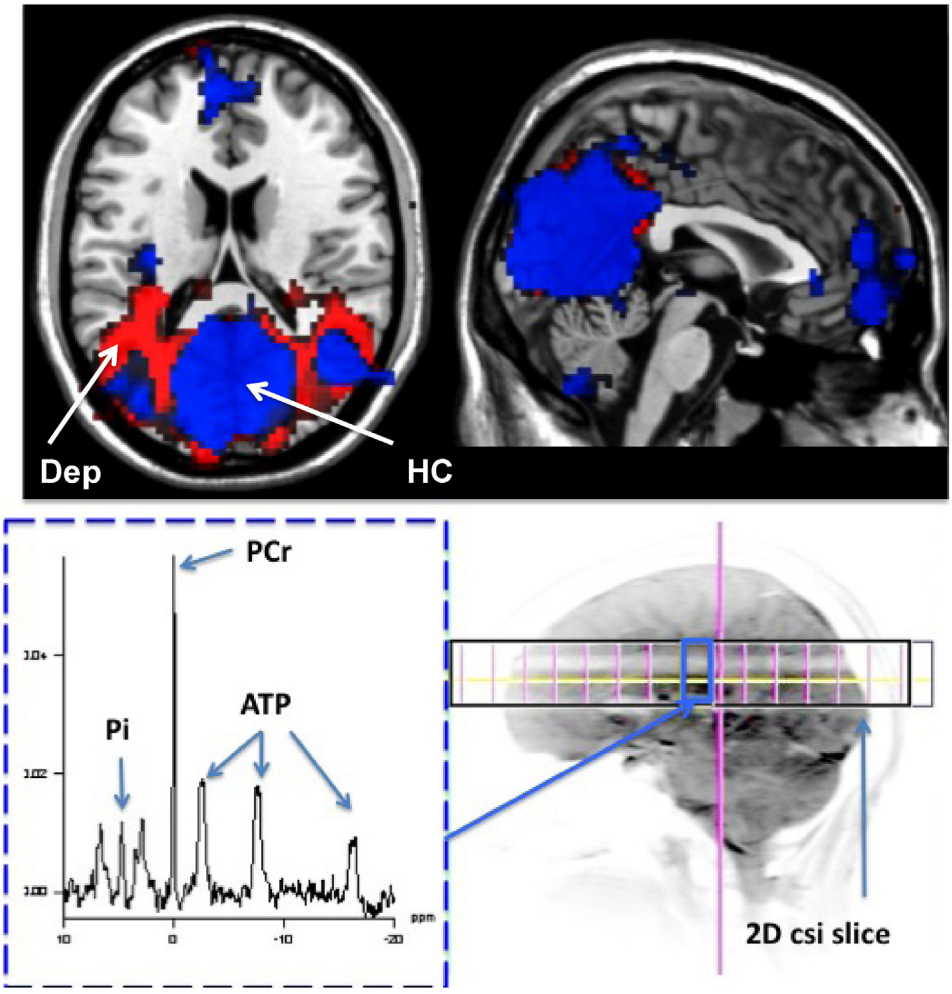

Fig. 2. Upper row (a): superimposed DMN activation maps of the HC (blue) and depressed patient (Dep, red) groups. Lower row (b): A typical ^{31}P spectrum extracted from a voxel in a 2D CSI slice at the midbrain and a sagittal view of a 2D CSI slice across the brain. The CSI was collected using a 1.28-ms hyperbolic sinc pulse for excitation and a 2D phase-encoding gradient matrix of 8 × 8 (weighted) and interpolated into 16 × 16 in post-processing. Other parameters included flip angle ~52°, TE = 2.3 ms, TR = 2.2 s, FOV = 220, and 18 signal averages for a total data acquisition time (TA) of 6.5 min.

3.3. Correlations

In the PCC region, the functional connectivity was not significantly correlated with regional Pi/PCr ratios ($p = 0.392$) for both groups. In the LPPC and RPPC regions, the functional connectivity of the healthy controls was negatively correlated ($p = 0.023$) with the regional Pi/PCr ratios (Fig. 4a) and its intercept on the Pi/PCr axis was 0.40 while those of the patient LPPC and RPPC were uncorrelated ($p = 0.867$). However, in the $LPPC_D$ and $RPPC_D$ regions, the functional connectivity of the patients was significantly and positively correlated with the regional Pi/PCr ratios (Fig. 4b) ($p = 0.0166$), with an intercept of 0.13 on the Pi/PCr axis. Similarly, normalized Pi (as calculated by Pi/(Pi + PCr)) was negatively correlated with regional connectivity of the LPPC and RPPC of the healthy controls and was positively correlated with the regional connectivity of the $LPPC_D$ and $RPPC_D$ of the patients. Normalized PCr was significantly lower in the $LPPC_D$ and $RPPC_D$ of the patients. However, there was no significant correlation between Pi/γATP and functional connectivity in the PCC and regions of the left posterior parietal cortex for both groups.

4. Discussion

The results of this preliminary study confirm that ^{31}P CSI can detect regional energy phosphates associated with DMN activity on a broadband clinical scanner and that these differences can be used to identify depressed patients from matched healthy controls. The major finding of this study is that the DMN of depressed patients was coherently and metabolically different from that of healthy controls. The difference appeared to be mainly in the bilateral posterior parietal cortex (Fig. 3) and was marked by the following key metrics: 1) higher resting state functional connectivity and lower Pi/γATP and Pi/PCr metabolic ratios, and 2) a distinct correlation between regional Pi/PCr ratios and functional connectivity.

The differences in coherence originated with the larger recruitment and the higher connectivity in the DMN regions of the posterior parietal cortex, especially in the left posterior parietal cortex (Fig. 3a, c), which has been found to be involved in a wide range of cognitive processes ranging from attention, memory, motor action and language to mathematical problem solving and social integration. Previous studies have shown that increased connectivity in parietal regions is associated with impaired emotional and cognitive processing such as deficits in attention, memory, and audiovisual emotional integration in depressed patients (Goveas et al., 2011; Müller et al., 2013). Resting state hyperconnectivity and larger recruitment of correlated regions in the DMN in depressed patients have also been observed in patients with MDD and are linked to depressive ruminations (Greicius et al., 2007; Berman et al., 2011; Hamilton et al., 2011). Following treatment with antidepressant medications, the hyperconnectivity of the DMN was reduced in depressed patients (Delaveau et al., 2011), which was associated with an improvement of their depressive symptoms.

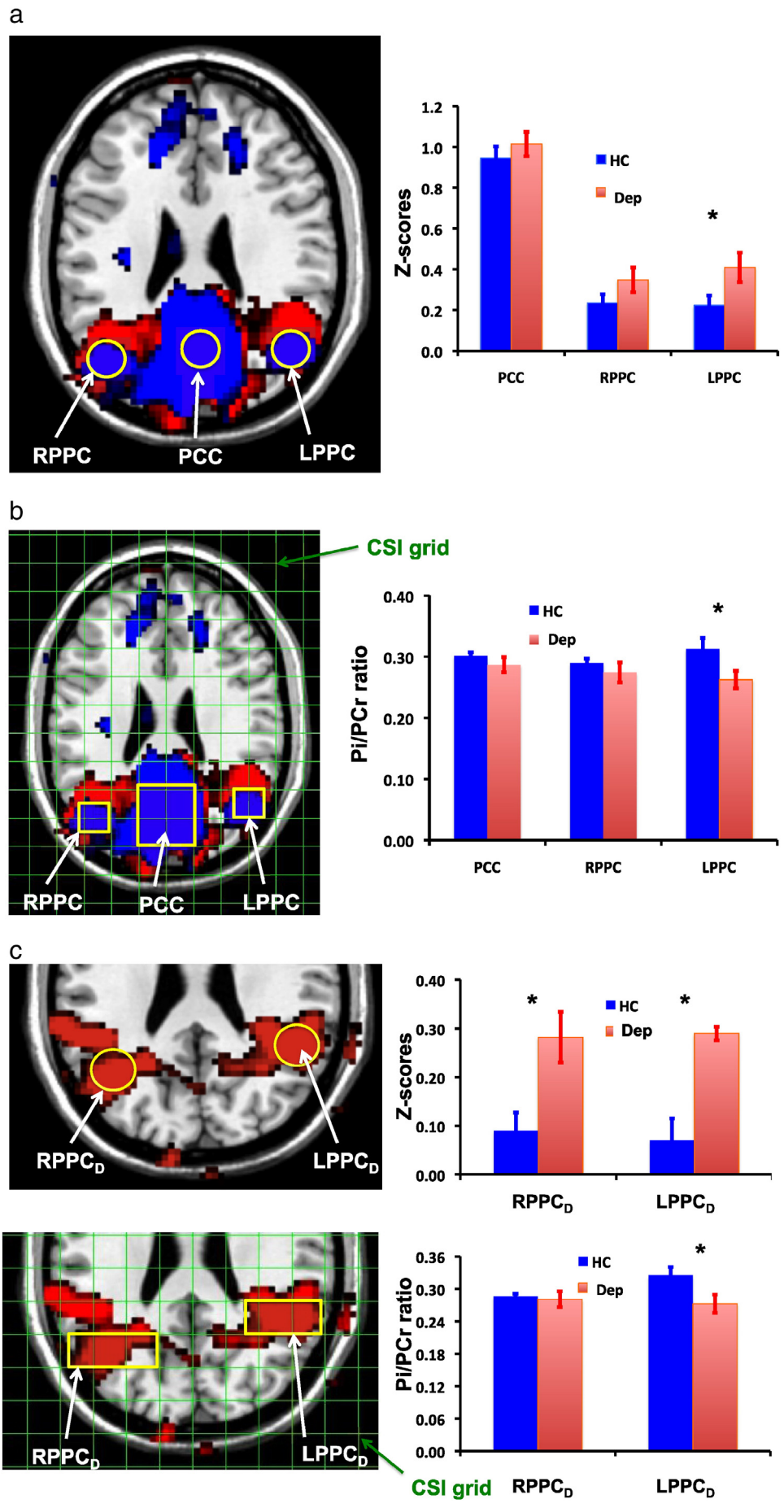
a
RPPC
PCC
LPPC
Z-scores
1.2
1.0
0.8
0.6
0.4
0.2
0.0
HC
Dep
*
PCC
RPPC
LPPC
b
CSI grid
RPPC
PCC
LPPC
Pi/PCr ratio
0.40
0.30
0.20
0.10
0.00
HC
Dep
*
PCC
RPPC
LPPC
c
RPPC$_D$
LPPC$_D$
Z-scores
0.40
0.30
0.20
0.10
0.00
*
*
HC
Dep
RPPC$_D$
LPPC$_D$
RPPC$_D$
LPPC$_D$
Pi/PCr ratio
0.36
0.30
0.24
0.18
0.12
0.06
0.00
HC
Dep
*
CSI grid
RPPC$_D$
LPPC$_D$

Table 3
Summary of pH and energy phosphate ratios measured in DMN regions.

	Summary of energy phosphate ratios measured in DMN regions				
Regions	Participant	Pi/PCr	Pi/γATP	PCr/mATP	pH
PCC	Dep	0.2775	**0.2447**	0.8360	6.9974
	HC	0.3035	**0.2770**	0.8604	6.9973
RPPC	Dep	0.2745	0.2604	0.8884	6.9935
	HC	0.2895	0.2727	0.9014	6.9899
LPPC	Dep	**0.2627**	**0.2382**	0.8421	7.0010
	HC	**0.3127**	**0.3000**	0.8614	7.0010
$RPPC_D$	Dep	0.2771	0.2646	0.8977	7.0096
	HC	0.2825	0.2636	0.8780	7.0009
$LPPC_D$	Dep	**0.2787**	**0.2573**	0.8739	6.9928
	HC	**0.3249**	**0.2925**	0.8438	6.9891

Where Dep = depressed patients and HC = healthy controls. Bold font indicates a statistically difference between the groups. PCr/mATP = 1/(average(αATP/PCr,γATP/PCr)).

By definition, hyperconnectivity represents a higher degree of coherence with the PCC seed region, which may or may not require a higher intensity of spontaneous BOLD MR signal. The Pi/PCr ratio is a quantity that links to ADP via equilibrium of creatine kinase reaction and a measure of phosphate energy stores compared to Pi. The ratio was shown to be a control factor in the work–biochemical cost relationship of functioning tissue and in oxidative phosphorylation of skeletal muscle (Chance et al., 1985; Chance et al., 1986). The negative correlation between Pi/PCr and functional connectivity (Z-scores) in the RPPC and LPPC regions of healthy controls suggests that regional connectivity is limited by the concentration and distribution of energy phosphates. The intercept on the Pi/PCr axis of Fig. 4a implies that if regional Pi/PCr reaches a level of 0.40 or beyond, then the regional resting-state connectivity would cease because all the available energy must be allocated to maintain the basic needs of the region. These data suggest that the regional DMN connectivity in the healthy controls does not rely on the regional PCr/Cr energy reservoir and is most likely supported by glycolysis and phosphorylation and was well regulated metabolically because during the resting state, oxygen and nutrition to the region via blood were at steady state and maintained regional protein synthesis and neural activity. The positive correlation in the RPPC and LPPC regions of the patients suggests that the connectivity in the LPPC and RPPC regions of the depressed brains most likely depends on the regional PCr/Cr reservoir, implicating a slower phosphorylation process in the regions. Future studies may offer more insight into the underlying mechanism that leads to the distinctive correlations of resting state functional connectivity and regional Pi/PCr between controls and depressed patients.

A few technical issues must be considered when mapping energy phosphates. First, ^{31}P CSI is subjected to chemical shift misregistration artifacts similar to proton spectroscopic imaging. In the present study, we set the carrier frequency at the PCr resonance and the chemical shift difference between Pi and PCr is approximately 5 ppm (approximately 240 Hz) yields about 7% of voxel misregistration error. While this error is tolerable for the present study, a larger excitation bandwidth or shifting carrier frequency may be needed when mapping other metabolites such as β-ATP, which is −16.3 ppm away from PCr. Second, we used the Pi/PCr ratio instead of absolute concentrations of the metabolites to minimize possible errors due to inhomogeneity of B_1 distribution across the brain. Future studies targeting quantitative measure of metabolite distribution should also take into account the flip angle, TR, and T1s of the metabolites to avoid possible saturation. As the apparent T1 of PCr is longer than that of Pi in vivo at 3 T (Blenman et al., 2006), overestimation of Pi/PCr values may occur when the flip angle is too high for a given TR. In addition, improving detection sensitivity of ^{31}P MRS and increasing spatial resolution for ^{31}P CSI in the future will improve the measurement accuracy of the activity/energy state relationship.

Finally, as with all studies of patients with a psychiatric disorder, medication effects must be considered. Obviously, unmedicated, depressed patients would have been ideal for a mechanism study, but such individuals are relatively rare, especially when older adults are included, and it would be unethical to ask a patient to delay starting their medication[s] in order to participate in this study, which targeted possible correlation between regional connectivity and energy metabolites. Instead, we elected to adopt inclusion/exclusion criteria that would admit only patients who were on stable doses of a limited number of

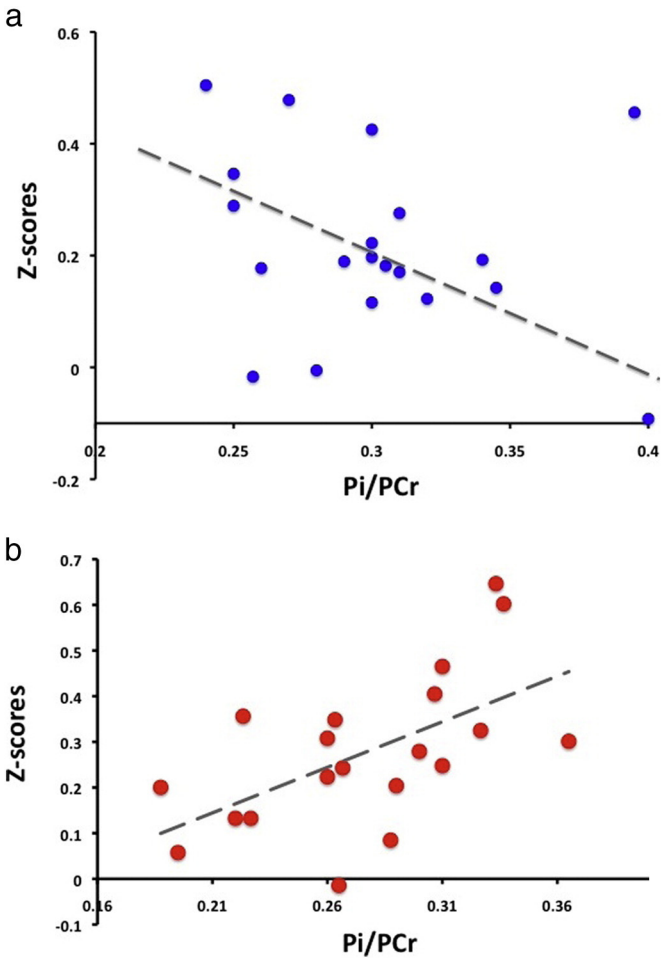

Fig. 4. a. Relationship between Pi/PCr ratios of RPPC and LPPC regions of healthy controls and the regional functional connectivity (Z-scores) observed in this study. Z = 0.818–2.0389 * (Pi/PCr), R^2 = 0.06, p = 0.023. b. Relationship between Pi/PCr ratios of $LPPC_D$ and $RPPC_D$ regions of the depressed patients and the regional functional connectivity (Z-scores) observed in the present study. Z = 1.892 * (Pi/PCr) − 0.2471, R^2 = 0.3352, p = 0.0166.

Fig. 3. a. Group averaged Z-scores (mean ± SE) in DMN regions of PCC and bilateral posterior parietal cortex (RPPC and LPPC) in Dep (red) and HC (blue). *p = 0.05. df = 22, t = 2.134, and the critical value is 2.074 (α = 0.05, two tails). b. Group averaged Pi/PCr ratios (mean ± SE) in DMN regions of PCC, RPPC, and LPPC in depressed patients (red) and HC (blue). The Pi/PCr ratios were extracted from CSI voxels (yellow boxes) at the corresponding anatomic locations in CSI map (green grid) superimposed on the group-averaged resting state correlation maps of healthy controls (blue) and depressed patients (red). Note the mildly lower Pi/PCr of patients compared to the healthy controls. *p < 0.05. df = 18, t = 2.164, critical value is 2.101 (α = 0.05, two tails). c. Summary of group averaged Z-scores (top row) and Pi/PCr ratios (lower row) (mean ± SE) in active regions ($RPPC_D$, $LPPC_D$) of posterior parietal cortex in depressed patients (depressed, red) compared to the controls (HC, blue). The ROIs (yellow circles and boxes) were selected from the difference of Z maps between the Dep and HC (red area = patient–HC). Note that the Z-scores of the patients were significantly higher than the controls and the significantly lower Pi/PCr of the patients in the left posterior parietal cortex ($LPPC_D$) compared to the healthy controls. *p < 0.05. For the connectivity (Z-scores) comparison, df = 22, t = 3.011 for RPPCD, t = 4.616 for LPPD, and critical value is 2.819 (α = 0.01, two tails). For Pi/PCr ratio comparison, df = 18, t = 2.284, and critical value is 2.101 (α = 0.05, two tails).

antidepressants and mood stabilizers but not on supplements or medications that may alter the energy state. Regardless of the medication effect, patients still presented with depressive symptoms and elevated HAM-D scores. Thus, the present study demonstrates a proof of concept that resting state functional connectivity and regional energy phosphates were correlated using a multimodal imaging approach of ^{31}P MRS and ^{1}H fMRI.

In summary, we found an altered metabolic pattern in the default mode network of depressed patients compared to healthy controls. The depressed DMN nodes in the PCC and posterior parietal cortex displayed a hyper-connective state that was associated with lower Pi/PCr ratios compared to those of the controls. The connectivity of the LPPC and RPPC regions was distinctively correlated with the regional Pi/PCr ratio depending on the controls or the depressed patients, implicating a possible coupling between depressed behavior and regional energetic stress.

Acknowledgment

This work was supported by a grant from NIH (MH081076 to CSZ). We appreciate the advice from Drs. P. Renshaw, B. Forester, S. Lowen, G. Trksak, and Y. Tong, statistical advice from Dr. L. Valeri via the Harvard Catalyst Biostatistics Program, and technical assistance of B. Glaeser, S. Kim, M. Woodward, M. Molly, and C. Caine during the course of this study.

References

Arnold, D.L., Matthews, P.M., et al., 1984. Metabolic recovery after exercise and the assessment of mitochondrial function in vivo in human skeletal muscle by means of ^{31}P NMR. Magn. Reson. Med. 1 (3), 307–315. http://dx.doi.org/10.1002/mrm.19100103036571561.

Beckmann, C.F., Smith, S.M., 2004. Probabilistic independent component analysis for functional magnetic resonance imaging. I.E.E.E. Transactions Med. Imaging 23 (2), 137–152. http://dx.doi.org/10.1109/TMI.2003.82282114964560.

Berman, M.G., Peltier, S., et al., 2011. Depression, rumination and the default network. Soc. Cogn. Affect. Neurosci. 6 (5), 548–555. http://dx.doi.org/10.1093/scan/nsq08020855296.

Blenman, R.M., Port, J.D., et al., 2006. In vivo measurement of T1 relaxation times of ^{31}P metabolites in human brain at 3 T. ISMRM 14th Scientific Meeting & Exhibition, Seattle, WA, USA.

Buckner, R.L., Andrews-Hanna, J.R., et al., 2008. The brain's default network: anatomy, function, and relevance to disease. Ann. N. Y. Acad. Sci. 1124, 1–38. http://dx.doi.org/10.1196/annals.1440.01118400922.

Castellanos, F.X., Margulies, D.S., et al., 2008. Cingulate–precuneus interactions: a new locus of dysfunction in adult attention-deficit/hyperactivity disorder. Biol. Psychiatry 63 (3), 332–337. http://dx.doi.org/10.1016/j.biopsych.2007.06.02517888409.

Cataldo, A.M., McPhie, D.L., et al., 2010. Abnormalities in mitochondrial structure in cells from patients with bipolar disorder. Am. J. Pathol. 177 (2), 575–585. http://dx.doi.org/10.2353/ajpath.2010.08106820566748.

Chai, X.J., Whitfield-Gabrieli, S., et al., 2011. Abnormal medial prefrontal cortex resting-state connectivity in bipolar disorder and schizophrenia. Neuropsychopharmacology 36 (10), 2009–2017. http://dx.doi.org/10.1038/npp.2011.8821654735.

Chance, B., Leigh, J.S., et al., 1985. Control of oxidative metabolism and oxygen delivery in human skeletal muscle: a steady-state analysis of the work/energy cost transfer function. Proc. Natl. Acad. Sci. U. S. A. 82 (24), 8384–8388. http://dx.doi.org/10.1073/pnas.82.24.83843866229.

Chance, B., Leigh, J.S., et al., 1986. Multiple controls of oxidative metabolism in living tissues as studied by phosphorus magnetic resonance. Proc. Natl. Acad. Sci. U. S. A. 83 (24), 9458–9462. http://dx.doi.org/10.1073/pnas.83.24.94583467315.

Chen, W., Zhu, X.H., et al., 1997. Increase of creatine kinase activity in the visual cortex of human brain during visual stimulation: a ^{31}P magnetization transfer study. Magn. Reson. Med. 38 (4), 551–557. http://dx.doi.org/10.1002/mrm.19103804089324321.

Corbetta, M., Shulman, G.L., 2002. Control of goal-directed and stimulus-driven attention in the brain. Nat. Rev. Neurosci. 3 (3), 201–215. http://dx.doi.org/10.1038/nrn75511994752.

Delaveau, P., Jabourian, M., et al., 2011. Brain effects of antidepressants in major depression: a meta-analysis of emotional processing studies. J. Affect. Disord. 130 (1–2), 66–74. http://dx.doi.org/10.1016/j.jad.2010.09.03221030092.

Donahue, M.J., Near, J., et al., 2010. Baseline GABA concentration and fMRI response. Neuroimage 53 (2), 392–398. http://dx.doi.org/10.1016/j.neuroimage.2010.07.01720633664.

Erecińska, M., Silver, I.A., 1989. ATP and brain function. J. Cereb. Blood Flow Metab. 9 (1), 2–19. http://dx.doi.org/10.1038/jcbfm.1989.2.

Goveas, J., Xie, C., et al., 2011. Neural correlates of the interactive relationship between memory deficits and depressive symptoms in nondemented elderly: resting fMRI study. Behav. Brain Res. 219 (2), 205–212. http://dx.doi.org/10.1016/j.bbr.2011.01.00821238490.

Greicius, M.D., Flores, B.H., et al., 2007. Resting-state functional connectivity in major depression: abnormally increased contributions from subgenual cingulate cortex and thalamus. Biol. Psychiatry 62 (5), 429–437. http://dx.doi.org/10.1016/j.biopsych.2006.09.02017210143.

Hamilton, J.P., Furman, D.J., et al., 2011. Default-mode and task-positive network activity in major depressive disorder: implications for adaptive and maladaptive rumination. Biol. Psychiatry 70 (4), 327–333. http://dx.doi.org/10.1016/j.biopsych.2011.02.00321459364.

Hamilton, M., 1960. A rating scale for depression. J. Neurol. Neurosurg. Psychiatry 23 (1), 56–62. http://dx.doi.org/10.1136/jnnp.23.1.5614399272.

Hetherington, H.P., Spencer, D.D., et al., 2001. Quantitative ^{31}P spectroscopic imaging of human brain at 4 Tesla: assessment of gray and white matter differences of phosphocreatine and ATP. Magn. Reson. Med. 45 (1), 46–52. http://dx.doi.org/10.1002/1522-2594(200101)45:1<46::AID-MRM1008>3.0.CO;2-N11146485.

Hu, Y., Chen, X., et al., 2013. Resting-state glutamate and GABA concentrations predict task-induced deactivation in the default mode network. J. Neurosci. 33 (47), 18566–18573. http://dx.doi.org/10.1523/JNEUROSCI.1973-13.201324259578.

Kato, T., Kato, N., 2000. Mitochondrial dysfunction in bipolar disorder. Bipolar Disord. 2 (3 Pt 1), 180–190. http://dx.doi.org/10.1034/j.1399-5618.2000.020305.x11256685.

MacDonald, M.L., Naydenov, A., et al., 2006. Decrease in creatine kinase messenger RNA expression in the hippocampus and dorsolateral prefrontal cortex in bipolar disorder. Bipolar Disord. 8 (3), 255–264. http://dx.doi.org/10.1111/j.1399-5618.2006.00302.x16696827.

Moore, C.M., Christensen, J.D., et al., 1997. Lower levels of nucleoside triphosphate in the basal ganglia of depressed subjects: a phosphorous-31 magnetic resonance spectroscopy study. Am. J. Psychiatry 154 (1), 116–118. http://dx.doi.org/10.1176/ajp.154.1.116.

Müller, V.I., Cieslik, E.C., et al., 2014. Crossmodal emotional integration in major depression. Soc. Cogn. Affect. Neurosci. 9 (6), 839–848. http://dx.doi.org/10.1093/scan/nst05723576809.

Muthukumaraswamy, S.D., Edden, R.A.E., et al., 2009. Resting GABA concentration predicts peak gamma frequency and fMRI amplitude in response to visual stimulation in humans. Proc. Natl. Acad. Sci. 106 (20), 8356–8361. http://dx.doi.org/10.1073/pnas.0900728106.

Northoff, G., Walter, M., et al., 2007. GABA concentrations in the human anterior cingulate cortex predict negative BOLD responses in fMRI. Nat. Neurosci. 10 (12), 1515–1517. http://dx.doi.org/10.1038/nn2001.

Öngür, D., Lundy, M., et al., 2010. Default mode network abnormalities in bipolar disorder and schizophrenia. Psychiatry Res. Neuroimag. 183 (1), 59–68. http://dx.doi.org/10.1016/j.pscychresns.2010.04.008.

Raichle, M.E., MacLeod, A.M., et al., 2001. A default mode of brain function. Proc. Natl. Acad. Sci. 98 (2), 676–682. http://dx.doi.org/10.1073/pnas.98.2.676.

Raichle, M.E., Mintun, M.A., 2006. Brain work and brain imaging. Annu. Rev. Neurosci. 29 (1), 449–476. http://dx.doi.org/10.1146/annurev.neuro.29.051605.112819.

Shulman, G.L., Fiez, J.A., et al., 1997. Common blood flow changes across visual tasks: II. Decreases in cerebral cortex. J. Cogn. Neurosci. 9 (5), 648–663. http://dx.doi.org/10.1162/jocn.1997.9.5.648.

Shulman, R.G., Rothman, D.L., et al., 2004. Energetic basis of brain activity: implications for neuroimaging. Trends Neurosci. 27 (8), 489–495. http://dx.doi.org/10.1016/j.tins.2004.06.005.

Weissman, D.H., Roberts, K.C., et al., 2006. The neural bases of momentary lapses in attention. Nat. Neurosci. 9 (7), 971–978. http://dx.doi.org/10.1038/nn1727.

Young, R.C., Biggs, J.T., et al., 1978. A rating scale for mania: reliability, validity and sensitivity. Br. J. Psychiatry 133 (5), 429–435. http://dx.doi.org/10.1192/bjp.133.5.429.